Time Between the Maximum and the Minimum of a Stochastic Process

Francesco Mori, Satya N. Majumdar, and Grégory Schehr
LPTMS, CNRS, Université Paris-Sud, Université Paris-Saclay, 91405 Orsay, France

(Received 13 September 2019; published 15 November 2019)

We present an exact solution for the probability density function $P(\tau = t_{\min} - t_{\max}|T)$ of the time difference between the minimum and the maximum of a one-dimensional Brownian motion of duration T. We then generalize our results to a Brownian bridge, i.e., a periodic Brownian motion of period T. We demonstrate that these results can be directly applied to study the position difference between the minimal and the maximal heights of a fluctuating $(1+1)$-dimensional Kardar-Parisi-Zhang interface on a substrate of size L, in its stationary state. We show that the Brownian motion result is universal and, asymptotically, holds for any discrete-time random walk with a finite jump variance. We also compute this distribution numerically for Lévy flights and find that it differs from the Brownian motion result.

DOI: 10.1103/PhysRevLett.123.200201

The properties of extremes of a stochastic process or time series of a given duration T are of fundamental importance in describing a plethora of natural phenomena [1–5]. For example, this time series may represent the amplitude of earthquakes in a specific seismic region, the amount of yearly rainfall in a given area, the temperature records in a given weather station, etc. The study of extremes in such natural time series has gained particular relevance in the recent context of global warming in climate science [6–10]. Extremal properties also play an important role for stochastic processes that are outside the realm of natural phenomena. For example, in finance, a natural time series is the price of a stock for a given period [11–14]. Knowing the maximum or the minimum value of a stock during a fixed period is obviously important, but an equally important question is “When does the maximum (minimum) value of the stock occur within this period $[0, T]$?” Let $t_{\max}$ and $t_{\min}$ denote these times (see, e.g., Fig. 1). For a generic stochastic process, computing the statistics of $t_{\max}$ and $t_{\min}$ is a fundamental and challenging problem. The simplest and the most ubiquitous stochastic process is the one-dimensional Brownian motion (BM) of a given duration T for which the probability distribution function (PDF) of $t_{\max}$ can be computed exactly [15–18]:

$$P(t_{\max}|T) = \frac{1}{\pi\sqrt{t_{\max}(T-t_{\max})}}, \qquad 0 \le t_{\max} \le T. \qquad (1)$$

The cumulative distribution $\text{Prob}(t_{\max} < t|T) = (2/\pi)\sin^{-1}(\sqrt{t/T})$ is known as the celebrated arcsine law of Lévy [15]. By the symmetry of the BM, the distribution of $t_{\min}$ is also described by the same arcsine law [Eq. (1)]. In the past decades, the statistics of $t_{\max}$ has been studied for a variety of stochastic processes, going beyond BM. Examples include BM with drift [19,20], constrained BM [21–23] (such as the Brownian bridge and the Brownian excursion; see also [23,24] for the real space renormalization group method), Bessel processes [23], Lévy flights [17,25], the random acceleration process [26], fractional BM [27,28], run-and-tumble particles [29], etc. The statistics of $t_{\max}$ has also been studied in multiparticle systems, such as N independent BMs [30], as well as for N vicious walkers [31]. Moreover, the arcsine law and its generalizations have been applied in a variety of situations, such as in disordered systems [32], stochastic thermodynamics [33], finance [34,35], and sports [36].

Although the marginal distributions of $t_{\max}$ and $t_{\min}$ are given by the same arcsine law in Eq. (1) for a BM due its symmetry, one expects that $t_{\max}$ and $t_{\min}$ are strongly

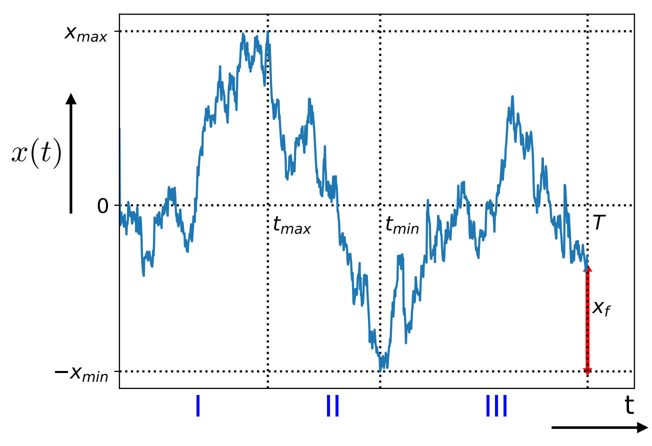

FIG. 1. Typical trajectory of Brownian motion $x(t)$ during time interval $[0, T]$, starting from $x(0) = 0$. The global maximum $x_{\max}$ occurs at time $t_{\max}$ and the global minimum $-x_{\min}$ at $t_{\min}$. The final position $x(T)$, measured with respect to $-x_{\min} \le 0$, is denoted by x_f. The total time interval $[0, T]$ is divided into three segments of $[0, t_{\max}]$ (I), $[t_{\max}, t_{\min}]$ (II), and $[t_{\min}, T]$ (III) for the case of $t_{\min} > t_{\max}$.

correlated. For example, if the maximum occurs at a certain time, it is unlikely that the minimum occurs immediately after or before. These anticorrelations are encoded in the joint distribution $P(t_{\min}, t_{\max}|T)$, which does not factorize into two separate arcsine laws. These anticorrelations also play an important role for determining the statistics of another naturally important observable, namely, the time difference between $t_{\min}$ and $t_{\max}$: $\tau = t_{\min} - t_{\max}$. In the context of finance, where the price of a stock is modeled by the exponential of a BM, τ represents the time difference between the occurrences of the minimum and the maximum of the stock price. For instance, if $t_{\max} < t_{\min}$ as in Fig. 1, an agent would typically sell her or his stock when the price is the highest and then wait an interval τ before rebuying the stock because the stock is the cheapest at time $t_{\min}$. Hence, a natural question is "How long should one wait between the buying and the selling of the stock?" In other words, one would like to know the PDF $P(\tau|T)$ of the time difference τ. To calculate this PDF, we need to know the joint distribution $P(t_{\min}, t_{\max}|T)$. Computing this joint distribution and the PDF $P(\tau|T)$ for a stochastic process is thus a fundamentally important problem.

In this Letter, by using a path-integral method, we compute the joint distribution $P(t_{\min}, t_{\max}|T)$ exactly for a BM of a given duration T. This joint distribution does not depend on the initial position x_0. Hence, without loss of generality, we set $x_0 = 0$. We also generalize our results to the case of a Brownian bridge (BB), which is a periodic BM of period T. Using these results, we first exactly compute the covariance function $\mathrm{cov}(t_{\min}, t_{\max}) = \langle t_{\min} t_{\max}\rangle - \langle t_{\min}\rangle\langle t_{\max}\rangle$ that quantifies the anticorrelation between $t_{\max}$ and $t_{\min}$. We find

$$\mathrm{cov}_{\mathrm{BM}}(t_{\min}, t_{\max}) = -\frac{7\zeta(3) - 6}{32} T^2 \approx -0.0754\ T^2$$

for a BM [with $\zeta(z)$ being the Riemann zeta function], whereas

$$\mathrm{cov}_{\mathrm{BB}}(t_{\min}, t_{\max}) = -\frac{\pi^2 - 9}{36} T^2 \approx -0.0241\ T^2$$

for a BB. From this joint distribution, we also exactly compute the PDF $P(\tau|T)$ for the BM, as well as for the BB. We show that, for a BM of duration T, starting at some fixed position, $P(\tau|T)$ has a scaling form for all τ and T: $P(\tau|T) = (1/T) f_{\mathrm{BM}}(\tau/T)$, where the scaling function $f_{\mathrm{BM}}(y)$ with $-1 \le y \le 1$ is given by

$$f_{\mathrm{BM}}(y) = \frac{1}{|y|}\sum_{m=1}^{\infty}(-1)^{m+1}\tanh^2\left(\frac{m\pi}{2}\sqrt{\frac{|y|}{1-|y|}}\right). \quad (2)$$

Clearly, $f_{\mathrm{BM}}(y)$ is symmetric around $y = 0$ but is nonmonotonic as a function of y (see Fig. 2, where we also compare it with numerical simulations, finding excellent agreement). This function has asymptotic behaviors

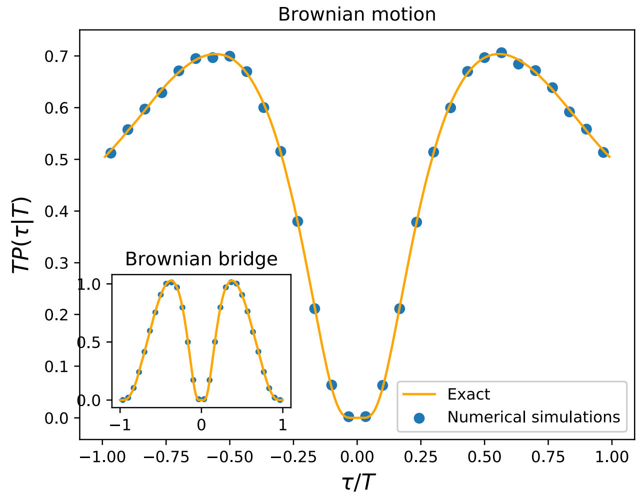

FIG. 2. Scaled distribution $TP(\tau|T)$ plotted as a function of τ/T for BM (solid line corresponds to exact scaling function $f_{\mathrm{BM}}(y)$ in Eq. (2), whereas filled dots are the results of simulations). Inset: the same scaled distribution for the Brownian bridge where the exact scaling function $f_{\mathrm{BB}}(y)$ is given in Eq. (4).

$$f_{\mathrm{BM}}(y) \underset{y\to 0}{\approx} \frac{8}{y^2} e^{-(\pi/\sqrt{y})}, \qquad f_{\mathrm{BM}}(y) \underset{y\to 1}{\approx} \frac{1}{2}. \quad (3)$$

For a BB, we get

$$f_{\mathrm{BB}}(y) = 3(1-|y|)\sum_{m,n=1}^{\infty}\frac{(-1)^{m+n} m^2 n^2}{[m^2|y| + n^2(1-|y|)]^{5/2}}, \quad (4)$$

which is again symmetric around $y = 0$ (see the inset of Fig. 2) and has the asymptotic behaviors

$$f_{\mathrm{BB}}(y) \underset{y\to 0}{\approx} \frac{\sqrt{2}\pi^2}{y^{9/2}} e^{-(\pi/\sqrt{y})}, \quad f_{\mathrm{BB}}(y) \underset{y\to 1}{\approx} \frac{\sqrt{2}\pi^2}{(1-y)^{7/2}} e^{-[\pi/(\sqrt{1-y})]}. \quad (5)$$

Next, we demonstrate that these scaling functions are universal in the sense of the central limit theorem. Indeed, consider a time series of n steps generated by the positions of a random walker evolving via the Markov rule

$$x_k = x_{k-1} + \eta_k, \quad (6)$$

starting from $x_0 = 0$, where η_k are independent and identically distributed random jump variables, with each drawn from a symmetric and continuous PDF $p(\eta)$. For all such jump distributions with a finite variance $\sigma^2 = \int \eta^2 p(\eta) d\eta$, we expect that, for large n, the corresponding PDF of the time difference of $\tau = t_{\min} - t_{\max}$ would converge to the same scaling function $f_{\mathrm{BM}}(y)$ as the BM. Similar result holds for the BB as well. We confirm this universality by an exact computation for

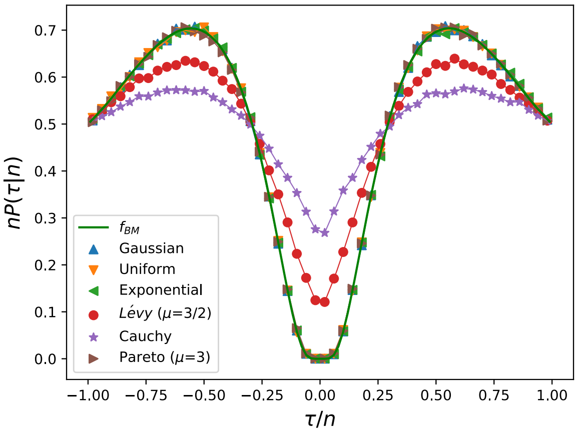

FIG. 3. Scaled distribution $nP(\tau|n)$ vs τ/n for random walks (RWs) with different jump distributions. The Gaussian, uniform, double-exponential, and Pareto (with index $\mu = 3$) jump distributions, all of which have a finite variance, collapse onto the Brownian scaling function $f_{\rm BM}(y)$ shown by the solid (green) line. For Lévy flights with index $\mu = 3/2$ and $\mu = 1$ (Cauchy distribution), the scaling function $f_\mu(y)$ depends on μ (except at the endpoints $y = \pm 1$, where $f_\mu(\pm 1) = 1/2$ seems to be universal for all $0 < \mu \leq 2$).

$p(\eta) = (1/2)e^{-|\eta|}$, and we do this numerically for other distributions with finite σ (see Fig. 3). In contrast, for Lévy flights, σ^2 is divergent because $p(\eta)$ has a heavy tail $p(\eta) \sim 1/|\eta|^{\mu+1}$ for large η, with an index of $0 < \mu < 2$. In this case, the PDF of τ is characterised by a different scaling function parametrized by μ that we compute numerically. Finally, we show how our results can be applied to study similar observables for heights in the stationary state of a Kardar-Parisi-Zhang (KPZ) or Edwards-Wilkinson (EW) interface in one dimension on a finite substrate of size L.

Brownian motion.—We start with a BM $x(t)$ over the time interval $t \in [0, T]$, starting at $x(0) = 0$ as in Fig. 1. Let $x_{\max} = x(t_{\max})$ and $-x_{\min} = x(t_{\min})$ denote the magnitude of the maximum and the minimum in [0, T]. Our strategy is to first compute the joint distribution $P(x_{\min}, x_{\max}, t_{\min}, t_{\max}|T)$ of these four random variables and then integrate out $x_{\max}$ and $x_{\min}$ to obtain the joint PDF $P(t_{\min}, t_{\max}|T)$. We note that, although the actual values $x_{\max}$ and $x_{\min}$ do depend on the starting position x_0, their locations $t_{\max}$ and $t_{\min}$ are independent of x_0 because it corresponds to a global shift in the position but not in time. The joint distribution of $x_{\max}$ and $x_{\min}$ can be computed by integrating out $t_{\max}$ and $t_{\min}$ (see, e.g., [37,38]). Without any loss of generality, we will assume that $t_{\max} < t_{\min}$ (the case $t_{\min} < t_{\max}$ can be analyzed in the same way). The grand joint PDF $P(x_{\min}, x_{\max}, t_{\min}, t_{\max}|T)$ can be computed by decomposing the time interval [0, T] into three segments: (I) $[0, t_{\max}]$, (II) $[t_{\max}, t_{\min}]$, and (III) $[t_{\min}, T]$. In the first segment (I), the trajectory starts at zero at time $t = 0$, arrives at $x_{\max}$ at time $t_{\max}$, and stays inside the space interval $x(t) \in [-x_{\min}, x_{\max}]$ during $[0, t_{\max}]$ (see Fig. 1). In the second segment (II), the trajectory starts at $x_{\max}$ at time $t_{\max}$ and arrives at $-x_{\min}$ at time $t_{\min}$, and it stays inside the box $[-x_{\min}, x_{\max}]$. Finally, in the third segment (III), the trajectory starts at $-x_{\min}$ at time $t_{\min}$ and stays inside the box $[-x_{\min}, x_{\max}]$ during $[t_{\min}, T]$. Clearly, the trajectory stays inside the box $[-x_{\min}, x_{\max}]$ because, by definition, it can neither exceed its maximum value $x_{\max}$ nor go below its minimum $-x_{\min}$. Let us also denote by $M = x_{\min} + x_{\max} \geq 0$.

To enforce the trajectory to stay inside the box, one needs to impose absorbing boundary condition at both $x_{\max}$ and $-x_{\min}$. However, for a continuous-time Brownian motion, it is well known that one cannot simultaneously impose an absorbing boundary condition and require the trajectory to arrive exactly at the absorbing boundary at a certain time. One way to get around this problem is to introduce a cutoff ϵ such that the actual values of the maximum and the minimum are, respectively, $x_{\max} - \epsilon$ and $-x_{\min} + \epsilon$; see Fig. S1 in the Supplemental Material (SM) [39]. One then computes the probability of the trajectory for a fixed ϵ and eventually takes the limit $\epsilon \to 0$. We use the Markov property of the process to express the total probability of the trajectory as the product of the probabilities of the three individual time segments. These probabilities can be expressed in terms of a basic building block or Green's function, which is defined as follows. Let $G_M(x, t|x_0, t_0)$ denote the probability density for a BM, starting at x_0 at t_0, to arrive at x at time t while staying inside the box $x(t) \in [0, M]$ during $[t_0, t]$. Note that $x, x_0 \in [0, M]$. This Green's function can be computed by solving the Fokker-Planck equation, $\partial_t G_M = (1/2)\partial_x^2 G_M$, with absorbing boundary conditions of $G_M = 0$ at both $x = 0$ and $x = M$ [46,47]:

$$G_M = \frac{2}{M}\sum_{n=1}^{\infty} \sin\left(\frac{n\pi x}{M}\right) \sin\left(\frac{n\pi x_0}{M}\right) e^{-[(n^2\pi^2)(t-t_0)/2M^2]}. \tag{7}$$

We first shift the origin in Fig. 1 to $-x_{\min}$. The probability of the trajectory in the three segments is then proportional, respectively, to (I) $G_M(M-\epsilon, t_{\max}|x_{\min}, 0)$, (II) $G_M(\epsilon, t_{\min}|M-\epsilon, t_{\max})$, and (III)

$$\int_0^M G_M(x_{\rm f}, T|\epsilon, t_{\min}) dx_{\rm f},$$

where, in the last segment, we integrate over the final position $x_{\rm f} = x(T) + x_{\min}$ of the trajectory inside the box $[0, M]$ (see Fig. 1). Hence, $P(x_{\min}, x_{\max}, t_{\min}, t_{\max}|T)$ is given, up to an overall normalization factor, by the product of three individual pieces. Using the Green's function in Eq. (7), one can explicitly compute this grand PDF and finally integrate over $x_{\max}$ and $x_{\min}$ to obtain the joint PDF $P(t_{\min}, t_{\max}|T)$ (see SM [39] for details). From the latter, we compute the covariance of $t_{\min}$ and $t_{\max}$ explicitly, as given above. Also, by integrating the joint PDF $P(t_{\min}, t_{\max}|T)$ over $t_{\max}$ and $t_{\min}$ with $t_{\min} - t_{\max} = \tau$ fixed, we explicitly compute the PDF $P(\tau|T)$ and find that it has the scaling form given in Eq. (2) [39].

Discrete-time random walks and Lévy flights.—It is natural to ask whether the PDF $P(\tau|T)$ of the continuous-time BM derived above holds for the discrete-time random walks or Lévy flights defined in Eq. (6). For such a discrete-time walk, let $n_{\max}$ ($n_{\min}$) denote the time at which the maximum (minimum) is reached. Remarkably, Sparre Andersen showed that the marginal distribution $P(n_{\max}|n)$ [equivalently $P(n_{\min}|n)$] is completely universal for all n, i.e., is the same for any symmetric jump PDF $p(\eta)$ [17]; thus, it is identical for random walks with both a finite jump variance and Lévy flights. In particular, for large n, $P(n_{\max}|n)$ converges to the arcsine law in Eq. (1), with T replaced by n and $t_{\max}$ replaced by $n_{\max}$. Does this universality also hold for the PDF of the time difference $\tau = n_{\min} - n_{\max}$? To investigate this question, we computed $P(\tau|n)$ exactly for the special case of a double exponential jump PDF $p(\eta) = (1/2)e^{-|\eta|}$. The details are left in the SM [39]; here, we just outline the main results. We find that, for large n, $P(\tau|n)$ converges to the scaling form $P(\tau|n) \approx (1/n)f_{\exp}(\tau/n)$, where $f_{\exp}(y)$ satisfies the integral equation

$$\int_0^1 dy \frac{f_{\exp}(y)}{1+uy} = \int_0^\infty dz \frac{2e^{-z}}{1-e^{-2z}} \tanh^2\left(\frac{z}{2\sqrt{1+u}}\right). \tag{8}$$

Remarkably, this integral equation can be solved; and we show $f_{\exp}(y) = f_{\rm BM}(y)$ obtained for the continuous-time BM in Eq. (2). This representation of $f_{\rm BM}(y)$ in Eq. (8) turns out to be useful to compute the moments of τ explicitly (see [39]). We would indeed expect this Brownian scaling form to hold for any jump densities with a finite variance σ^2 due to the central limit theorem. We have numerically verified this universality for other jump distributions $p(\eta)$ with a finite variance (see Fig. 3). However, for heavy tailed distributions, such as for Lévy flights with an index $0 < \mu < 2$, we numerically find that while, for large n, $P(\tau|n) \approx (1/n)f_\mu(\tau/n)$, the scaling function $f_\mu(y)$ depends on μ (see Fig. 3), except at endpoints $y = \pm 1$, where it seems that $f_\mu(\pm 1) = 1/2$ independently of $0 < \mu \le 2$. The result for $P(\tau = n_{\min} - n_{\max}|n)$ is thus less universal as compared to the marginal distributions of $n_{\max}$ and $n_{\min}$ given by the arcsine laws [Eq. (1)].

Brownian bridge.—We now turn to the statistics of $t_{\max}$ and $t_{\min}$ for a BB where the initial position of $x(0) = 0$ and the final position of $x(T) = 0$ are identical. The motivation for studying the BB comes from the fact that this will be directly applicable to study KPZ or EW interfaces with periodic boundary conditions in space (see below). For the BB, it is well known [16] that $P(t_{\max}|T) = 1/T$, i.e., uniform over $t_{\max} \in [0, T]$. The same result holds for $t_{\min}$ as well. However, we find that the PDF of their difference of $\tau = t_{\min} - t_{\max}$ takes the scaling form $P(\tau|T) = (1/T)f_{\rm BB}(\tau/T)$ for all T, where the scaling function $f_{\rm BB}(y)$ is nontrivial as in Eq. (4). To derive this result, we follow the same path decomposition method as in the case of the BM, except in the third segment $t \in [t_{\min}, T]$, where we need to impose that the final position of the trajectory is $x(T) = 0$. Thus, while in time segments (I) and (II) the probabilities are exactly the same for the BM and the BB, in segment (III) we have simply $G_M(x_{\min}, T|\epsilon, t_{\min})$ for the BB (after the shift of the origin to $-x_{\min}$). Taking the product of the three segments, and following the same calculations as in the BM case (see [39]), we obtain the result for $f_{\rm BB}(y)$ in Eq. (4). As shown in the SM [39], this result can also be alternatively derived by exploiting a mapping, known as Vervaat's construction [48], between the BB and the Brownian excursion (the latter being just a BB constrained to stay positive on [0, T]). We have also verified these calculations by simulating a BB using an algorithm proposed in Ref. [49], finding excellent agreement (see Fig. 2).

Fluctuating interfaces.—Our results can be applied directly to $(1+1)$-dimensional KPZ or EW interfaces. Consider a one-dimensional interface growing on a finite substrate of length L, with $H(x,t)$ denoting the height of the interface at position x and time t, with $0 \le x \le L$ [50–52]. We study both free and periodic boundary conditions (FBC and PBC, respectively). In the former case, the heights at the endpoints of $x = 0$ and $x = L$ are free, whereas in the latter case, $H(0,t) = H(L,t)$. The height field evolves by the KPZ equation [53]

$$\frac{\partial H(x,t)}{\partial t} = \frac{\partial^2 H(x,t)}{\partial x^2} + \lambda\left(\frac{\partial H(x,t)}{\partial x}\right)^2 + \eta(x,t), \tag{9}$$

where $\lambda \ge 0$, and $\eta(x,t)$ is a Gaussian white noise with zero mean and correlator $\langle \eta(x,t)\eta(x',t')\rangle = 2\delta(x-x')\delta(t-t')$. The zero mode, i.e., the spatially averaged height

$$\overline{H(t)} = (1/L)\int_0^L H(x,t)dx,$$

typically grows with time. Hence, the PDF of $H(x,t)$ does not reach a stationary state, even for a finite system. However, the distribution of the relative heights $h(x,t) = H(x,t) - \overline{H(t)}$ does reach a stationary state at long times for finite L. For the simpler case of the EW [54] interface [$\lambda = 0$ in Eq. (9)], the joint PDF of the stationary relative height $h(x)$ in the case of the FBC is given by [55–57]

$$P_{\rm st}(\{h\}) = B_L e^{-1/2\int_0^L dx(\partial_x h)^2}\delta\left(\int_0^L h(x)dx\right). \tag{10}$$

Here, B_L is a normalization constant, and the delta function enforces the zero area constraint

$$\int_0^L h(x)dx = 0,$$

which follows from the definition of the relative height. Incidentally, this result for the FBC holds also for the KPZ equation with $\lambda > 0$, but only in the large L limit. Thus, locally, the stationary height field $h(x)$ for $\lambda \geq 0$ is a BM in space, with x playing the role of time. For the PBC, an additional factor of $\delta[h(0) - h(L)]$ is present in Eq. (10) (see Refs. [55–57]); moreover, it holds for any finite L and arbitrary $\lambda \geq 0$ [39]. The PDF of the maximal relative height $h_{\max} = \max_{0\leq x\leq L} h(x)$ was computed exactly for both boundary conditions [55,56]. These distributions are nontrivial due to the presence of the global constraint of zero area under the BM or BB. Under the correspondences $x \Leftrightarrow t$, $L \Leftrightarrow T$, and $h(x) \Leftrightarrow x(t)$, the stationary interface maps onto a BM (for FBC) and to a BB (for PBC) of duration T, but with an important difference: the corresponding BM and BB have a zero-area constraint. Although this constraint affects the PDF of the maximal (minimal) height, it is clear that the position at which the maximal (respectively, minimal) height occurs is not affected due to this global shift by the zero mode. Hence, the distributions of the positions of maximal and minimal heights for the stationary KPZ or EW interface are identical to that of $t_{\max}$ and $t_{\min}$ for the BM (for FBC) and the BB (for PBC). Hence, the PDF of $\tau = t_{\min} - t_{\max}$ given in Eqs. (2) and (4) also gives the PDF of the position difference between the minimal and maximal heights in the stationary KPZ/EW interface. We have verified this analytical prediction for the KPZ or EW interfaces by solving Eq. (9) numerically, finding excellent agreement (see figures 4 and 5 in [39]).

We have presented an exactly solvable example for the distribution of the time difference between the occurrences of the maximum and the minimum of a stochastic process of a given duration T. Our results show that, even for BM or BB, this distribution is highly nontrivial. We have also shown how the same distribution shows up for KPZ or EW interfaces in $1+1$ dimensions in their stationary state. Computing this non-trivial distribution for other stochastic processes, such as Lévy flights, remains a challenging open problem.

[1] E. J. Gumbel, *Statistics of Extremes* (Dover, New York, 1958).

[2] R. W. Katz, M. B. Parlange, and P. Naveau, Adv. Water Resour. **25**, 1287 (2002).

[3] R. W. Katz, G. S. Brush, and M. B. Parlange, Ecology **86**, 1124 (2005).

[4] J. Krug, J. Stat. Mech. (2007) P07001.

[5] J. Neidhart and J. Krug, Phys. Rev. Lett. **107**, 178102 (2011).

[6] S. Redner and M. R. Petersen, Phys. Rev. E **74**, 061114 (2006).

[7] S. Rahmstorf and D. Coumou, Proc. Natl. Acad. Sci. U.S.A. **108**, 17905 (2011).

[8] B. Christiansen, J. Clim. **26**, 7863 (2013).

[9] G. Wergen, A. Hense, and J. Krug, Clim. Dyn. **42**, 1275 (2014).

[10] S. N. Majumdar, P. von Bomhard, and J. Krug, Phys. Rev. Lett. **122**, 158702 (2019).

[11] J.-P. Bouchaud and M. Potters, *Theory of Financial Risks. From Statistical Physics to Risk Management* (Cambridge University Press, Cambridge, England, 2000).

[12] M. Yor, *Exponential Functionals of Brownian Motion and Related Processes* (Springer Science & Business Media, New York, 2001).

[13] P. Embrechts, C. Klüppelberg, and T. Mikosch, *Modelling Extremal Events: For Insurance and Finance* (Springer Science & Business Media, New York, 2013), Vol. 33.

[14] D. Challet, Appl. Math. Finance **24**, 1 (2017).

[15] P. Lévy, Compos. Math. **7**, 283 (1940).

[16] W. Feller, *Introduction to Probability Theory and Its Applications* (John Wiley & Sons, New York, 1950).

[17] E. Sparre Andersen, Math. Scand. **1**, 263 (1953).

[18] P. Mörters and Y. Peres, *Brownian Motion* (Cambridge University Press, Cambridge, England, 2010), Vol. 30.

[19] E. Buffet, J. Appl. Math. Stoch. Anal. **16**, 201 (2003).

[20] S. N. Majumdar and J.-P. Bouchaud, Quant. Finance **8**, 753 (2008).

[21] J. Randon-Furling and S. N. Majumdar, J. Stat. Mech. (2007) P10008.

[22] S. N. Majumdar, J. Randon-Furling, M. J. Kearney, and M. Yor, J. Phys. A **41**, 365005 (2008).

[23] G. Schehr and P. Le Doussal, J. Stat. Mech. (2010) P01009.

[24] P. Le Doussal and C. Monthus, Physica (Amsterdam) **317A**, 140 (2003).

[25] S. N. Majumdar, Physica (Amsterdam) **389A**, 4299 (2010).

[26] S. N. Majumdar, A. Rosso, and A. Zoia, J. Phys. A **43**, 115001 (2010).

[27] M. Delorme and K. J. Wiese, Phys. Rev. E **94**, 052105 (2016).

[28] T. Sadhu, M. Delorme, and K. J. Wiese, Phys. Rev. Lett. **120**, 040603 (2018).

[29] P. Singh and A. Kundu, J. Stat. Mech. (2019) P083205.

[30] S. N. Majumdar, A. Comtet, and J. Randon-Furling, J. Stat. Phys. **138**, 955 (2010).

[31] J. Rambeau and G. Schehr, Phys. Rev. E **83**, 061146 (2011).

[32] S. N. Majumdar, A. Rosso, and A. Zoia, Phys. Rev. Lett. **104**, 020602 (2010).

[33] A. C. Barato, É. Roldàn, I. A. Martínez, and S. Pigolotti, Phys. Rev. Lett. **121**, 090601 (2018).

[34] C. Dale and R. Workman, Financ. Anal. J. **36**, 71 (1980).

[35] J. Baz and G. Chacko, *Financial Derivatives: Pricing, Applications, and Mathematics* (Cambridge University Press, Cambridge, England, 2004).

[36] A. Clauset, M. Kogan, and S. Redner, Phys. Rev. E **91**, 062815 (2015).

[37] A. Kundu, S. N. Majumdar, and G. Schehr, Phys. Rev. Lett. **110**, 220602 (2013).

[38] S. N. Majumdar, S. Sabhapandit, and G. Schehr, Phys. Rev. E **94**, 062131 (2016).

[39] See Supplemental Material at http://link.aps.org/supplemental/10.1103/PhysRevLett.123.200201 for details of the computations, which includes Refs. [40–45].
[40] S. N. Majumdar, Brownian functionals in physics and computer science, in The Legacy Of Albert Einstein: A Collection of Essays in Celebration of the Year of Physics (World Scientific, 2007), p. 93.
[41] V. V. Ivanov, Astron. Astrophys. **286**, 328 (1994).
[42] S. N. Majumdar, P. Mounaix, and G. Schehr, J. Stat. Mech. (2014) P09013.
[43] N. I. Muskhelishvili, *Singular Integral Equations, Boundary Problems of Function Theory and Their Application to Mathematical Physics* (Dept. of Supply and Development, Aeronautical Research Laboratories, Melbourne, 1949).
[44] C.-H. Lam and F. G. Shin, Phys. Rev. E **57**, 6506 (1998).
[45] C.-H. Lam and F. G. Shin, Phys. Rev. E **58**, 5592 (1998).
[46] H. Risken, *The Fokker-Planck Equation* (Springer, Berlin, 1996).
[47] S. Redner, *A Guide to First-Passage Processes* (Cambridge University Press, Cambridge, England, 2001).
[48] W. Vervaat, Ann. Probab. **7**, 143 (1979).
[49] S. N. Majumdar and H. Orland, J. Stat. Mech. (2015) P06039.
[50] T. Halpin-Healy and Y. C. Zhang, Phys. Rep. **254**, 215 (1995).
[51] J. Krug, Adv. Phys. **46**, 139 (1997).
[52] H. Spohn, in *Stochastic Processes and Random Matrices*, edited by G. Schehr, A. Altland, Y. V. Fyodorov, and L. F. Cugliandolo, Lecture Notes of the Les Houches Summer School, Vol. 104, (Oxford University Press, Oxford, 2015).
[53] M. Kardar, G. Parisi, and Y.-C. Zhang, Phys. Rev. Lett. **56**, 889 (1986).
[54] S. F. Edwards and D. R. Wilkinson, Proc. R. Soc. A **381**, 17 (1982).
[55] S. N. Majumdar and A. Comtet, Phys. Rev. Lett. **92**, 225501 (2004).
[56] S. N. Majumdar and A. Comtet, J. Stat. Phys. **119**, 777 (2005).
[57] G. Schehr and S. N. Majumdar, Phys. Rev. E **73**, 056103 (2006).